30th Congress of the International Council
of the Aeronautical Sciences
DCC, Daejeon, Korea ; September 25-30, 2016

PERCH LANDING ASSISTED BY THRUSTER (PLAT): SIX D.O.F TRAJECTORY OPTIMIZATION

Seungyeop Han*, Byung-Yoon Lee*, Jaemyung Ahn* and Min-Jea Tahk
*** Korea Advanced Institude of Science and Technology**

Keywords: *Vertical Landing, Thrusters Assisted, Deep Stall, Trajectory Optimization*

Abstract

This paper handles a trajectory optimization of fixed wing aircraft perch landing assisted by thruster. The paper develops aircraft model and deals with six-degree-of-freedom motion for further understanding of dynamic phenomena of proposed landing method. The landing maneuver is described as an optimal control problem minimizing the fuel consumption with specified terminal landing conditions. The optimal solution is computed by Gauss Pseudo Spectral Method (GPM) and realistic possibility of the method is validated based on the optimized solution.

1 Introduction

Unmanned Aerial Vehicles (UAV) systems are increasingly used throughout the regions where securing a runway is almost impossible such as mountain or marine area. General fixed wing airplanes are inherently required a long distance runway due to their approach velocity, which must be above the stall speed. Recently, many landing methods have been suggested to overcome the flaw of fixed wing airplane.

Among them, Tahk [1] proposed the patent about the new landing concept that can be applied up to medium size UAVs. The proposed concept named as PLAT (Perch Landing Assisted by Thruster) use both aerodynamic drag and thruster to reduce the velocity effectively and to land at desired position precisely. Patent divide the PLAT maneuver into three phase; approach phase, deep stall phase and thrusting phase sequentially. The idea is similar to well known 'Soft lunar landing' optimal control problem [10] in that the thrusters are used, but is different from the Lunar soft landing by the use of an aero-breaking maneuver.

A realistic possibility of PLAT landing is verified through researches [2-5]. Work of [4-5] transcribe PLAT maneuver into the optimal control problem with two-dimensional point mass dynamics. In their works, an objective is set as minimizing the overall thruster input, to unsure the amount of propellant requirements during landing and the optimal solutions are computed via Euler-Lagrange method and Gauss-Pseudo-spectral Method (GPM). Paper of [2-3] further developed the result of [4-5] by considering pitch dynamics and adopting more realistic aerodynamic model. Through these researches optimal landing method is obtained and required propellant mass are approximately computed with some assumptions.

The biggest improvement of the paper is model extension. Compare to the previous works limited on longitudinal motion only, both longitudinal and lateral motions are considered for trajectory optimization. Therefore extended modeling method for inertia and aerodynamic modeling are also introduced.

The rest of paper is organized as follows. Detail description of new concept, modeling of reference aircraft and modeling of high angle of attack aerodynamic are introduced at Section 2. In Section 3, formulation of optimal control problem including cost function, dynamic equations and boundary conditions and optimization results with analysis of the results are presented. Lastly, Section 4 covers concluding remarks as well as introduces a future work.

2 Perch Landing Assisted by Thruster

The section introduces detail explanation of suggested method PLAT and aircraft that will be used for simulation, modeling procedures. Some of following contents are referred of paper [1-5].

2.1 PLAT Description [1-5]

The three phases of PLAT (approach phase, deep stall phase, and thrusting phase) and the thruster configuration required for this approach are presented in Fig. 1 and Fig. 2, respectively. To accomplish the proposed landing method, configuration composed of the two thrusters at the left/right wing for lateral control and the two at the front/back fuselage for longitudinal control is proposed.

The proposed landing maneuver on phases are elucidated as follows and further details can be find at the research [1-5]. During approach phase, vehicle approaches the desired landing position horizontally. While the aircraft is in the deep stall phase, thrusters create large pitch up moment and will be controlled to retain proper pitch angle that makes the largest possible drag. Lastly, four thrusters will propel the aircraft upward to accomplish a soft land in thrusting phase. In case where lateral offset between current aircraft position and desired landing spot exist, lateral shift maneuver is required during landing. To do that, lateral thrusters and control surfaces will be used, as shown in Fig. 3.

2.2 Aircraft Modeling

For PLAT simulation, some parameters of the unmanned aerial vehicle 'RQ-7B Shadow 200', which is conventional fixed wing type aircraft with high wing, constant chord and pusher configuration, are used. As details of parameters are unavailable, those are estimated via approximated three dimensional model as shown in Fig. 4.

2.2.1 Inertia Modeling

To estimate the mass property such as center of mass and moment of inertia, aircraft model is divided into four parts; main wing, tail wing, body and twin-boom. Based on existing data of the UAV and existing works [6], mass portion of each subpart is set as $m_{wing} = 0.4m_{A/C}$, $m_{tail} = 0.15m_{A/C}$, $m_{body} = 0.2m_{A/C}$ and $m_{boom} = 0.2m_{A/C}$. Software program 'Solidworks' is used to construct three dimensional model and to compute mass inertia. Details of aircraft parameters after 3D model estimation are listed at Table 1.

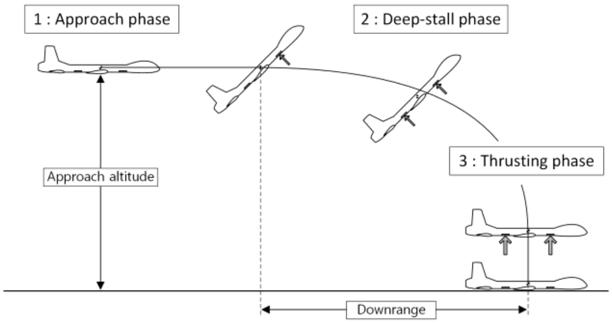

Fig. 1. PLAT Maneuver Concept

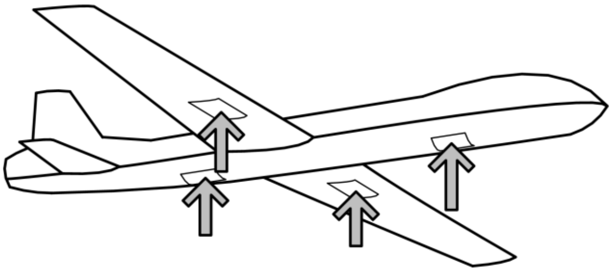

Fig. 2. Thruster Configuration

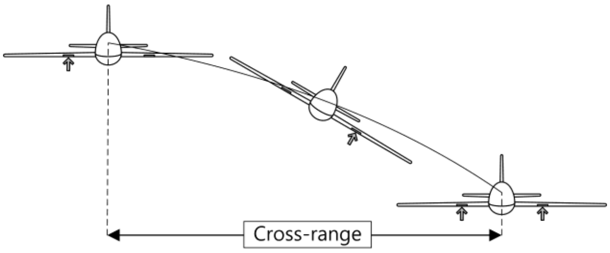

Fig. 3. PLAT Maneuver for Lateral Correction

2.2.2 Aerodynamic Modeling

Airfoil of the main wing and tail wing of 'RQ-7B Shadow 200' are respectively assumed to be NACA4415 and NACA0015. Aero data at high angle of attack are required to approximate the PLAT method accurately. At Fig. 6-7, experimental static aerodynamic coefficient data of each airfoil is marked. Both information of NACA4415 and NACA0015 at high angle of attack are known from research [7] and [8].

Aircraft Parameter		Value [unit]
m	*Gross weight*	$140\,\mathrm{kg}$
I_{xx}	*X-axis moment of inertia*	$82.59\,\mathrm{kg\cdot m^2}$
I_{yy}	*Y-axis moment of inertia*	$99.07\,\mathrm{kg\cdot m^2}$
I_{zz}	*Z-axis moment of inertia*	$174.07\,\mathrm{kg\cdot m^2}$
I_{xz}	*XZ product of inertia*	$10.63\,\mathrm{kg\cdot m^2}$
c_w	*Main wing chord length*	0.610 m
b_w	*Main wing wingspan*	4.300 m
S_w	*Main wing area*	2.623 $\mathrm{m^2}$
AR_w	*Main Aspect Ratio*	7.0492
x_w	*Main wing AC-CG length*	0.1725 m
y_w	*Main wing AC-CG length*	1.075 m
z_w	*Main wing AC-CG length*	0.075 m
c_h	*H-tail chord length*	0.390 m
b_h	*H-tail wingspan*	1.320 m
S_h	*H-tail area*	0.515 $\mathrm{m^2}$
AR_h	*H-tail Aspect Ratio*	3.385
x_h	*H-tail AC-CG length*	1.783 m
z_h	*H-tail AC-CG length*	0.240 m
c_v	*V-tail chord length*	0.390 m
b_v	*V-tail wingspan*	0.380 m
S_v	*V-tail area*	0.296 $\mathrm{m^2}$
AR_v	*V-tail Aspect Ratio*	1.949
x_v	*V-tail AC-CG length*	1.783 m
z_v	*V-tail AC-CG length*	0.240 m
i_w	*Main wing incidence angle*	3 deg
i_h	*H-tail incidence angle*	-1 deg
d_x	*Lon Thruster arm length*	0.5 m
d_y	*Lat Thruster arm length*	0.5 m

Table. 1. ‘RQ-7B Shadow 200’ 3D Model Data

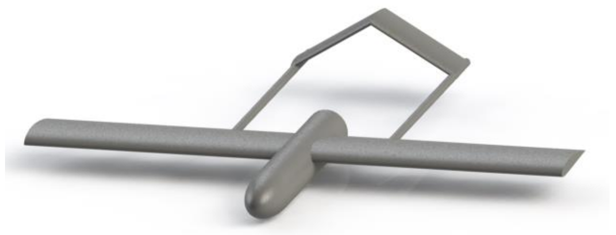

Fig. 4. ‘RQ-7B Shadow 200’ 3D Model

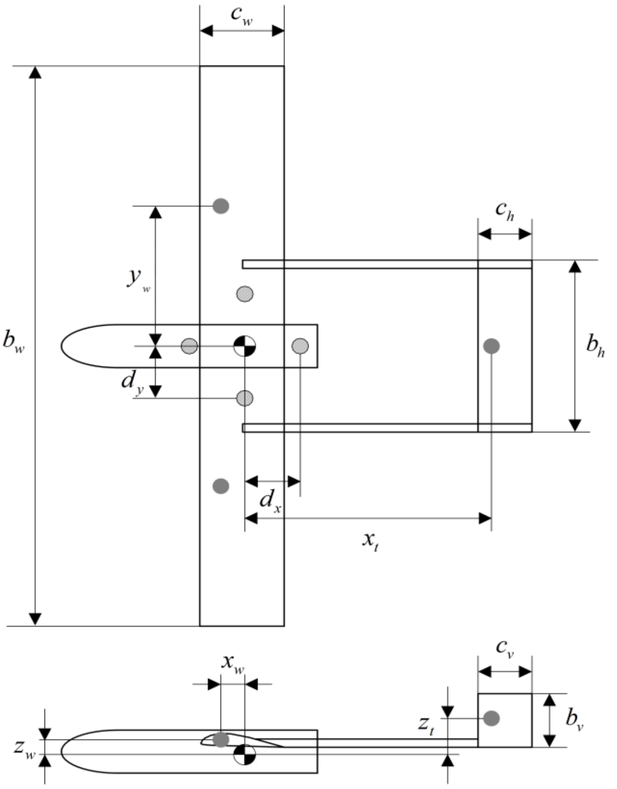

Fig. 5. ‘RQ-7B Shadow 200’ 3D Model Top & Side View

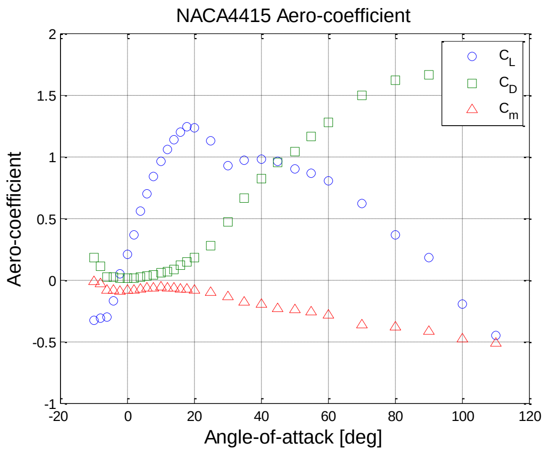

Fig. 6. NACA4415 Aero-Coefficient Plot

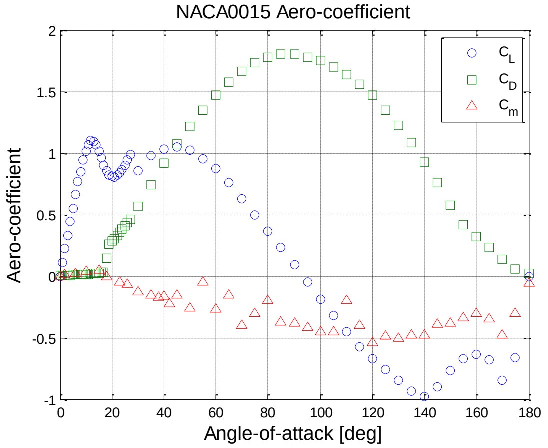

Fig. 7. NACA0015 Aero-Coefficient Plot

To include aerodynamic variation due to body angular velocity, this paper adopts same method used in [2,3]. The method is computing a local angle of attack for each subpart separately with respect to its own aerodynamic center.

For given body velocity $\mathbf{v}_{cg}^{B}$, body angular velocity $\boldsymbol{\omega}_{B/I}^{B}$ and relative displacement between subpart aerodynamic center to aircraft center of mass $\mathbf{r}_{X}^{B}$, local velocity at subpart aerodynamic center can be computed as (1). In here subscript ξ denotes for subpart (main wing, h-tail, v-tail) and superscript B denotes for body frame.

$$\mathbf{v}_{\xi}^{B} = \mathbf{v}_{cg}^{B} + \boldsymbol{\omega}_{B/I}^{B} \times \mathbf{r}_{\xi}^{B} \tag{1}$$

Assuming that only tangential airflow has an effect on the aerodynamic forces, results the equation for local angle of attack as (2) and corresponding aerodynamic forces as (3).

$$\begin{aligned}
\alpha_{w,r} &= \operatorname{atan2}\left(\left(\mathbf{v}_{w,r}^{B}\right)_3, \left(\mathbf{v}_{w,r}^{B}\right)_1\right) + i_w \\
\alpha_{w,l} &= \operatorname{atan2}\left(\left(\mathbf{v}_{w,l}^{B}\right)_3, \left(\mathbf{v}_{w,l}^{B}\right)_1\right) + i_w \\
\alpha_{h} &= \operatorname{atan2}\left(\left(\mathbf{v}_{h}^{B}\right)_3, \left(\mathbf{v}_{h}^{B}\right)_1\right) + i_h \\
\alpha_{v} &= \operatorname{atan2}\left(\left(\mathbf{v}_{v}^{B}\right)_3, \left(\mathbf{v}_{v}^{B}\right)_2\right)
\end{aligned} \tag{2}$$

$$\begin{aligned}
L_{\xi} &= Q_{\xi} S_{\xi} C_{L_{\xi}}\left(\alpha_{\xi}\right) \\
D_{\xi} &= Q_{\xi} S_{\xi}\left(C_{D_{\xi}}\left(\alpha_{\xi}\right) + \frac{C_{L_{\xi}}{}^{2}\left(\alpha_{\xi}\right)}{\pi e AR_{\xi}}\right) \\
M_{\xi} &= Q_{\xi} c_{\xi} S_{\xi} C_{m_{\xi}}\left(\alpha_{\xi}\right)
\end{aligned} \tag{3}$$

Once aerodynamic forces and moments from each subpart are known, adding them properly based on the aircraft geometry reveals the total aerodynamic external forces and moments as in (4).

$$\begin{aligned}
X_{aero} &= \sum_{\xi} X_{\xi}\left(L_{\xi}, D_{\xi}, \alpha_{\xi}\right), & L_{aero} &= \sum_{\xi} L_{\xi}\left(L_{\xi}, D_{\xi}, \alpha_{\xi}, \mathbf{x}_{\xi}\right) \\
Y_{aero} &= \sum_{\xi} Y_{\xi}\left(L_{\xi}, D_{\xi}, \alpha_{\xi}\right), & M_{aero} &= \sum_{\xi} M_{\xi}\left(L_{\xi}, D_{\xi}, \alpha_{\xi}, \mathbf{x}_{\xi}\right) \\
Z_{aero} &= \sum_{\xi} Z_{\xi}\left(L_{\xi}, D_{\xi}, \alpha_{\xi}\right), & N_{aero} &= \sum_{\xi} N_{\xi}\left(L_{\xi}, D_{\xi}, \alpha_{\xi}, \mathbf{x}_{\xi}\right)
\end{aligned} \tag{4}$$

2.3 Modeling Assumptions

Body aerodynamic effects are ignored and aerodynamic variation caused by angular velocity is considered only. In addition, the solid propellant rocket is assumed to be have following two properties: 1) the level of thrust is continuous, and 2) the thruster can be switched on and off repeatedly.

3 Trajectory Optimization

3.1 Optimal Control Problem Formulation

The amount of propellant requirement during landing is one of the most important things not sure to validate the realistic possibility of the suggested landing method, PLAT. In that sense, the objective function is formulated to minimize the overall thruster input as (5).

$$J = \int_{t_0}^{t_f} \left(T_f + T_b + T_l + T_r\right) dt \tag{5}$$

Governing aircraft equations of motion in six degrees of freedom is given as (6). In case of external forces and moments, equations are given as (7).

$$\begin{aligned}
\dot{u} &= rv - qw + T_{L/B}(3,1) g + f_x \\
\dot{v} &= pw - ru + T_{L/B}(3,2) g + f_y \\
\dot{w} &= qu - pv + T_{L/B}(3,3) g + f_z \\
\begin{bmatrix} \dot{p} \\ \dot{q} \\ \dot{r} \end{bmatrix} &= [I]^{-1} \begin{bmatrix} L_m - \left(I_{zz} - I_{yy}\right) qr + I_{xz} pq \\ M_m - \left(I_{xx} - I_{zz}\right) pr - I_{xz}\left(p^2 - r^2\right) \\ N_m - \left(I_{yy} - I_{xx}\right) pq - I_{xz} qr \end{bmatrix} \\
\begin{bmatrix} \dot{X} \\ \dot{Y} \\ \dot{Z} \end{bmatrix} &= T_{L/B} \begin{bmatrix} u \\ v \\ w \end{bmatrix} \\
\begin{bmatrix} \dot{q}_0 \\ \dot{q}_1 \\ \dot{q}_2 \\ \dot{q}_3 \end{bmatrix} &= \frac{1}{2} \begin{bmatrix} 0 & -p & -q & -r \\ p & 0 & r & -q \\ q & -r & 0 & p \\ r & q & -p & 0 \end{bmatrix} \begin{bmatrix} q_0 \\ q_1 \\ q_2 \\ q_3 \end{bmatrix}
\end{aligned} \tag{6}$$

$$T_{L/B} = \begin{bmatrix} q_0^2 + q_1^2 - q_2^2 - q_3^2 & 2\left(q_1 q_2 - q_0 q_3\right) & 2\left(q_1 q_3 + q_0 q_2\right) \\ 2\left(q_1 q_2 + q_0 q_3\right) & q_0^2 - q_1^2 + q_2^2 - q_3^2 & 2\left(q_2 q_3 - q_0 q_1\right) \\ 2\left(q_1 q_3 - q_0 q_2\right) & 2\left(q_2 q_3 + q_0 q_1\right) & q_0^2 - q_1^2 - q_2^2 + q_3^2 \end{bmatrix}$$

$$\begin{aligned}
f_x &= \frac{1}{m} X_{aero} \\
f_y &= \frac{1}{m} Y_{aero} \\
f_z &= \frac{1}{m}\left(Z_{aero} - T_f - T_b - T_r - T_l\right) \\
L_m &= L_{aero} + T_l d_y - T_r d_y \\
M_m &= M_{aero} + T_f d_x - T_b d_x \\
N_m &= N_{aero}
\end{aligned} \tag{7}$$

The initial conditions for PLAT maneuver is set as trimmed conditions for level flight. The terminal velocity and angular velocity of the vehicle must be near zero when altitude is zero to land softly. Above boundary conditions can be described as set of equality and inequality constraints. Due to page limit, such constraints are omitted, but can be check through result graph at later sections.

3.2 Optimization Results

The pseudo-spectral method (PSM) is used to solve the formulated optimal control problem. The PSM parametrizes both of control and state vectors at selected collocation points and thereby converts a dynamic optimization problem to a nonlinear programming problem. The optimal control problem was implemented in MATLAB and GPOPS-II is used to solve the problem [9].

3.2.1 PLAT without cross-range

Optimization results with zero cross-range are plotted through Fig. 8 to Fig. 12. From the Fig 8 and 9, both linear and angular velocity of aircraft become zero when it does touch-down. From Fig 10 and 12, thrusters are properly used for pitching up and retaining maneuver. Except for the retaining maneuver interval, Bang-off-Bang likes control is found.

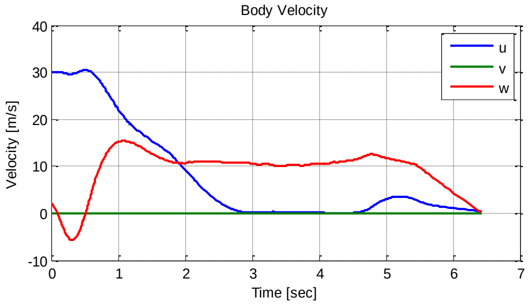

Fig. 8. Body Velocity Components History

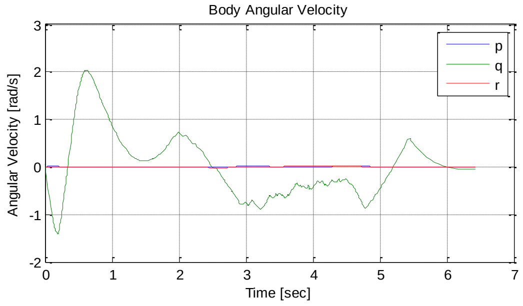

Fig. 9. Body Angular Velocity Components History

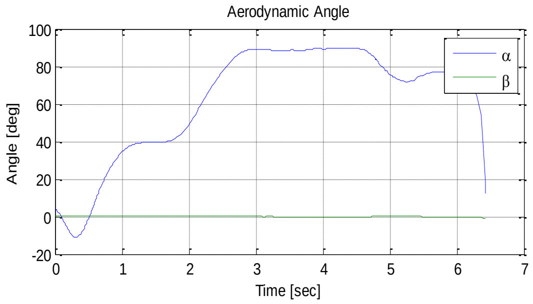

Fig. 10. Aerodynamic Angle History

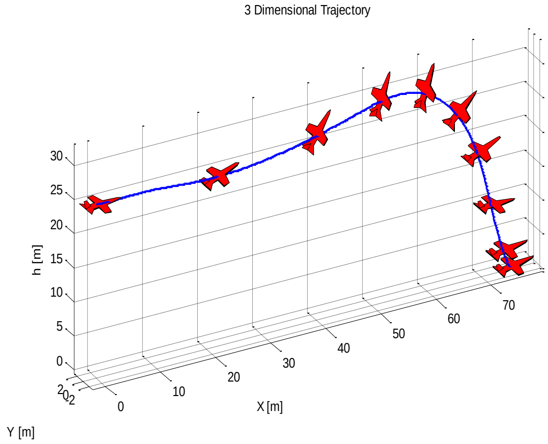

Fig. 11. PLAT Maneuver 3D Trajectory

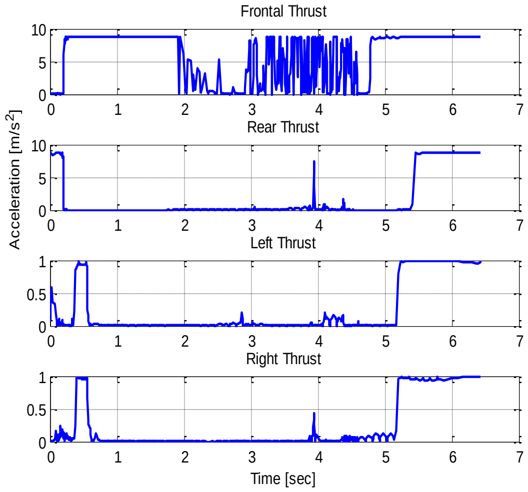

Fig. 12. Thrust Control History

3.2.2 PLAT with cross-range

Optimization results with nonzero cross-range are plotted through Fig. 13 to Fig. 17. As previous, terminal landing criteria for velocity are satisfied. Likewise, Bang-off-Bang likes control is found except for the retaining maneuver interval.

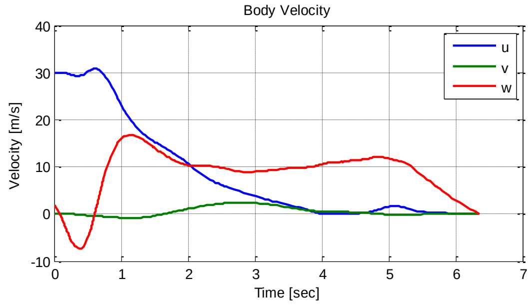

Fig. 13. Body Velocity Components History

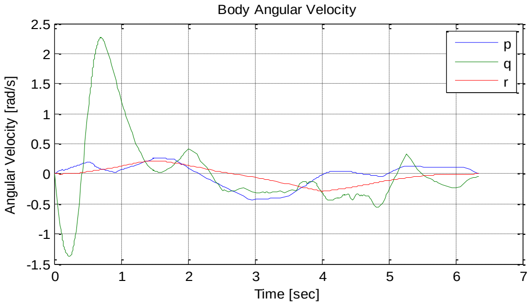

Fig. 14. Body Angular Velocity Components History

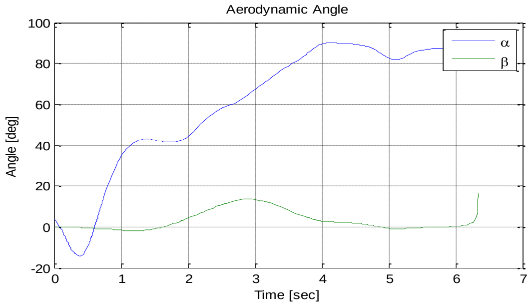

Fig. 15. Aerodynamic Angle History

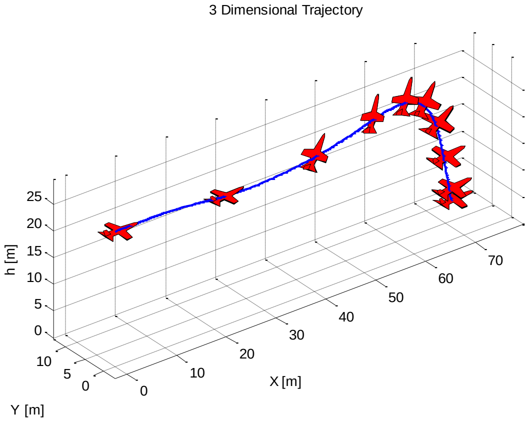

Fig. 16. PLAT Maneuver 3D Trajectory

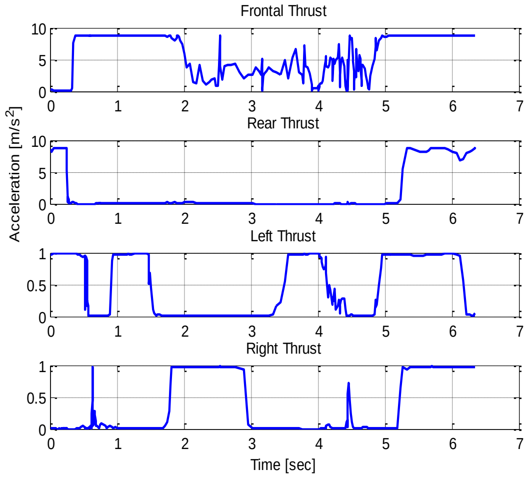

Fig. 17. Thrust Control History

3.2.3 PLAT Analysis

Analogously to results from previous work [2-5], the optimal result concludes Bang-off-Bang control as a fuel minimizing control. Physical meaning of computed optimal cost is the total impulse generated from thruster. From following equation (8). Each scenario requires $5930\,\mathrm{N \cdot s}$ and $6000\,\mathrm{N \cdot s}$ amount of total impulse respectively to accomplish the PLAT maneuver.

$$J^* = \int_0^{t_f} \sum T\,dt = I^* = Isp \cdot m_{fuel}^* \cdot g \qquad (8)$$

If solid rocket propellants which generally has specific impulse around $240\,\mathrm{sec}$ are used for PLAT system, then overall required propellant mass is about $2.52\,\mathrm{kg}$ and $2.55\,\mathrm{kg}$ respectively.

4 Conclusion

Trajectory optimization of six degrees of freedom motion based PLAT with approximated aircraft parameters is conducted. Based on the optimized results, the PLAT can make the aircraft land at the desired spot with several terminal criteria.

Although the solutions dignify the proposed method, there exist some critical limitations. Such as assumption of continuous and repeatable thrusters and problems on real world implementation are long way to be studied. But still, the paper has meaningful to suggest and validate the new way of landing for fixed wing.

5 References

[1] Tahk M J, Lee B Y and Han S Y. *Method and System of Vertical Take-Off and Landing for Unmanned Aerial Vehicle*, Korean Patent 10-2015-0015295, 2014.

[2] Tahk M J, Han S Y, Lee B Y and Ahn J M. Trajectory optimization and Control Algorithm of Longitudinal Perch Landing Assisted by Thruster, *Proceeding of European Control Conferences*, Denmark, 2016.

[3] Tahk M J, Han S Y, Lee B Y and Ahn J M. Perch Landing Assisted by Thruster (PLAT): Concept and Trajectory Optimization. *International Journal of Aeronautical and Space Sciences*, submitted for review, 2016.

[4] Han, S.Y., Tahk, M.J., and Ahn, J.M.: “Perch Landing Assisted by Thruster”, Proceedings of the KSAS Spring Conferences, Jeongseon Korea, 2015.

[5] Han S Y, Yogaswara Y H, Lee B Y, Tahk M J and Ahn J M. Trajectory Optimization of Longitudinal Perch Landing Assisted by Thruster, *Proceedings of the 12th YUST International Symposium*, Yanbian China, 2015.

[6] Douglas Cau. Simulation of search over terrain with unmanned aerial vehicles, *AIAA Infotech@Aerospace Conference*, St. Louis MO, 2011.

[7] Ostowari C, and Naik D. *Post-Stall Wind Thnnel Data for NACA 44XX Series Airfoil Sections*, Solar Energy Research Institute, 1985.

[8] Sheldahl R E, and Klimas P C. *Aerodynamic Characteristics of Seven Symmetrical Airfoil Sections through 180-Degree Angle of Attack for Use in Aerodynamic Analysis of Vertical Axis Wind Turbines*, Sandia National Laboratories Rept. SAND80-2114, 1981.

[9] Michael A Patterson, Anil V Rao, GPOPS-II: A MATLAB Software for Solving Multiple-Phase Optimal Control Problems Using hp-Adaptive Gaussian Quadrature Collocation Methods and Sparse Nonlinear Programming, *ACM Transactions on Mathematical Software (TOMS)*, v.41 n.1, p.1-37, October 2014.

[10] Kirk D E. *Optimal Control Theory; An Introduction*, Dover, New York, pp. 247-248, 1970.

Copyright Statement

The authors confirm that they, and/or their company or organization, hold copyright on all of the original material included in this paper. The authors also confirm that they have obtained permission, from the copyright holder of any third party material included in this paper, to publish it as part of their paper. The authors confirm that they give permission, or have obtained permission from the copyright holder of this paper, for the publication and distribution of this paper as part of the ICAS proceedings or as individual off-prints from the proceedings.